http://dx.doi.org/10.5012/bkcs.2013.34.9.2573

Articles

Effect of Manganese Vanadate Formed on the Surface of Spinel Lithium Manganese Oxide Cathode on High Temperature Cycle Life Performance

Jun-Il Kim,† Sun-Min Park,† Kwang Chul Roh,† and Jae-Won Lee*

*Department of Energy Engineering, Dankook University, Cheonan 330-714, Korea. *E-mail: jwlee7@dankook.ac.kr*
†Energy Materials Center, Korea Institute of Ceramic Engineering & Technology, Seoul 153-801, Korea
Received February 7, 2013, Accepted April 9, 2013

Rate capability and cyclability of $LiMn_2O_4$ should be improved in order to use it as a cathode material of lithium-ion batteries for hybrid-electric-vehicles (HEV). To enhance the rate capability and cyclability of $LiMn_2O_4$, it was coated with MnV_2O_6 by a sol–gel method. A V_2O_5 sol was prepared by a melt-quenching method and the $LiMn_2O_4$ coated with the sol was heat-treated to obtain the MnV_2O_6 coating layer. Crystal structure and morphology of the samples were examined by X-ray diffraction, SEM and TEM. The electrochemical performances, including cyclability at 60 °C, and rate capability of the bare and the coated $LiMn_2O_4$ were measured and compared. Overall, MnV_2O_6 coating on $LiMn_2O_4$ improves the cyclability at high temperature and rate capability at room temperature at the cost of discharge capacity. The improvement in cyclability at high temperature and the enhanced rate capability is believed to come from the reduced contact between the electrode, and electrolyte and higher electric conductivity of the coating layer. However, a dramatic decrease in discharge capacity would make it impractical to increase the coating amount above 3 wt %.

Key Words : Lithium-ion battery, $LiMn_2O_4$, MnV_2O_6 coating, Cyclability, Rate capability

Introduction

$LiMn_2O_4$ is one the most promising cathode materials, along with $LiFePO_4$, for HEV power source due to its low cost, safety and good power capability. However, this material suffers from Mn-dissolution at high temperature into the electrolyte, causing poor cycle life and storage performance.[1,2] To solve this problem, metal doping at the Mn-sites, minimization of the surface area in contact with the electrolyte with adequate morphology control, and surface coating with various metal oxides have been tried with success.[3-5] The coating of electrically insulating materials such as alumina or magnesia improved the high temperature cyclability, but degraded the rate capability, which is another important requirement for high power source applications.[6,7] Moreover, CeO_2, SiO_2, ZrO_2, ZnO, TiO_2, AlF_3 coatings have been applied on $LiMn_2O_4$ with much success on enhancing the cycling stability.[8-14] Highly electronic conductive oxide like ITO (indium tin oxide) or other lithium-ion insertion materials such as $FePO_4$ has been adopted as the coating material.[15,16] Recently, V_2O_5 coating on $LiCoO_2$ has been applied for improving the cycle life performance.[17] V_2O_5 coating is considered as one of the most efficient surface treatment for the cathode materials as V_2O_5 sol can be easily prepared with a simple melt-quenching process. In this study, V_2O_5 was coated on $LiMn_2O_4$ and calcined to obtain $LiMn_2O_4$ covered with MnV_2O_6 particles *via* a simple sol-gel process. The effect on the electrochemical performance, including cycle life performance at high temperature and rate capability at room temperature, were investigated.

Experimental

$LiMn_2O_4$ was prepared by solid-state reaction, for which 10 mol % excess lithium hydroxide and electrolytic manganese dioxide (MnO_2) were mixed by ball milling. The mixture was calcined at 1000 °C in air for 12 h with a heating and cooling rate of 5 °C min^{-1}. Then, the $LiMn_2O_4$ was coated with MnV_2O_6 using a sol-gel process. A V_2O_5 sol was prepared by melt quenching.[18] The crystalline V_2O_5 powder was melted at 800 °C in an electric furnace for 20 min, then quenched in distilled water with vigorous stirring. A brownish sol was obtained after 2 h and the appropriate amount of $LiMn_2O_4$ was dipped into the sol. The mixture was stirred continuously at 80 °C and finally the sol was transformed into a gel. The gel on the $LiMn_2O_4$ was dried at 70 °C in a convection oven for 8 h and then heat-treated at 400 °C for 12 h in air. Coating concentration (wt %) was calculated with the solid V_2O_5 in the sol and $LiMn_2O_4$.

The crystal structure of the obtained powder was analyzed by powder X-ray diffraction (XRD, Rigaku D/Max-2500/PC) using a Cu Kα radiation source. The particle size and shape of the samples were examined by field emission-scanning microscopy (FE-SEM, S-800, Hitachi). The coating status of the sample was observed by transmission electron microscopy (TEM, JEM 2000EX, JEOL).

Coin-cells (CR2016) were used to determine the electrochemical performance of the obtained samples. A positive electrode was made by coating a slurry of the active material, Super-P carbon black (MMM), and a polyvinylidene fluoride (PVdF) binder (Kurea) at a weight ratio of 80:10:10 onto an aluminum foil current collector. The coin-cells, containing a cathode, lithium foil as an anode and a reference electrode, and a microporous polyethylene separator, were assembled in an argon-filled glove box. The electrolyte used was a 1.0 M $LiPF_6$ solution in ethylene carbonate/ethyl-methyl carbonate (EC/EMC) (1/2 vol %) (Cheil Ind., Korea). The galvanostatic charge and discharge cycle tests of the cell were carried out at room temperature and 60 °C between 3.0 V and 4.3 V.

Results and Discussion

The XRD peak patterns of the bare and MnV_2O_6-coated $LiMn_2O_4$ are shown in Figure 1. The peaks for MnV_2O_6 become higher with increasing coating concentration. The coated $LiMn_2O_4$ without heat treatment did not exhibit any peaks for MnV_2O_6 (not shown here). These results suggested that MnV_2O_6 is formed during the heat treatment by the reaction between the V_2O_5 sol and $LiMn_2O_4$. The lattice constants for the bare and coated $LiMn_2O_4$, given in the inset of Figure 1, decrease with increasing coating concentration, which indicates that a part of vanadium ions is diffused into the $LiMn_2O_4$ lattice and occupies the Mn-site to form a solid solution during the heat treatment even at 400 °C.

It is expected that the manganese ions can be easily replaced by vanadium ions and the lattice constant of the doped material will decrease because the ionic radius of V^{5+} (68 pm) is smaller than that of Mn^{3+} (72 pm) and similar to that of Mn^{4+} (67 pm).

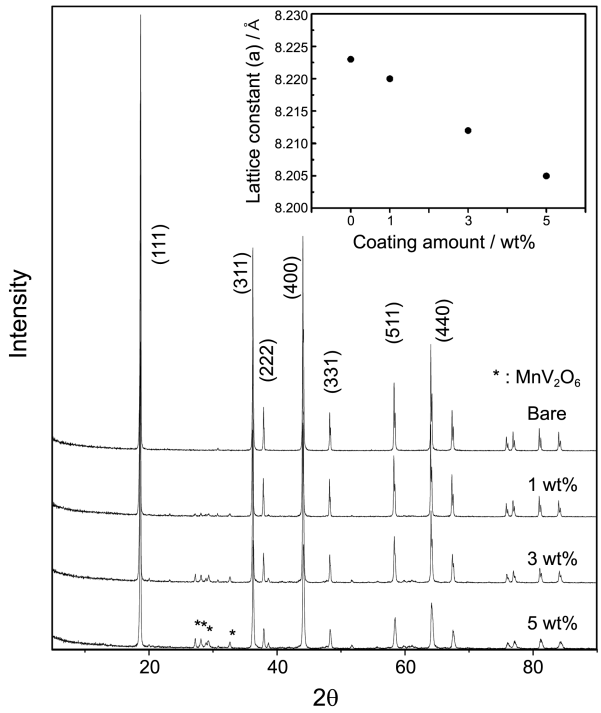

Figure 1. XRD peak patterns of the bare and MnV_2O_6-coated $LiMn_2O_4$ (Inset: Lattice constants).

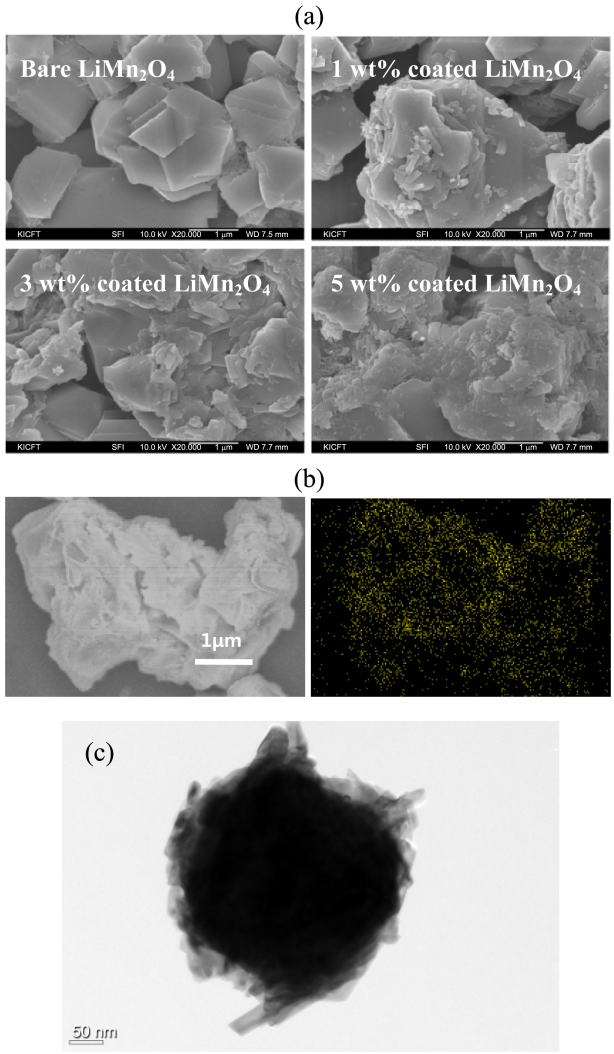

Figure 2. (a) SEM images of the bare and MnV_2O_6-coated $LiMn_2O_4$, (b) vanadium-mapping for 5 wt % MnV_2O_6-coated $LiMn_2O_4$ by EDS, and (c) TEM images of 5 wt % MnV_2O_6-coated $LiMn_2O_4$.

Figure 2(a) shows the morphology of the sample. The bare $LiMn_2O_4$ has an octahedral shape with smooth surface which disappears gradually with increasing coating concentration.

The uniform distribution of the coating material was confirmed from the vanadium mapping image for the 5 wt %-coated sample by energy dispersive X-ray spectroscopy (EDS) (Figure 2(b)). TEM image (Figure 2(c)) reveals that the coating layer is not a continuous film but composed of the nanorod aggregates of MnV_2O_6. The coating layer partly covers the surface of the $LiMn_2O_4$ particles and appears irregular. The thickness of the coating layer is approximately 50 nm.

Figure 3 presents the rate capability of the samples measured at room temperature. The rate capability was improved with increasing coating concentration at the cost of decreased capacity. The capacity retention rate at 2 C-rate *vs.* 0.1 C-rate was 87.5, 89.0, 95.0, 97.5% for the bare, 1, 3, 5 wt % coated sample respectively. Despite the excellent rate

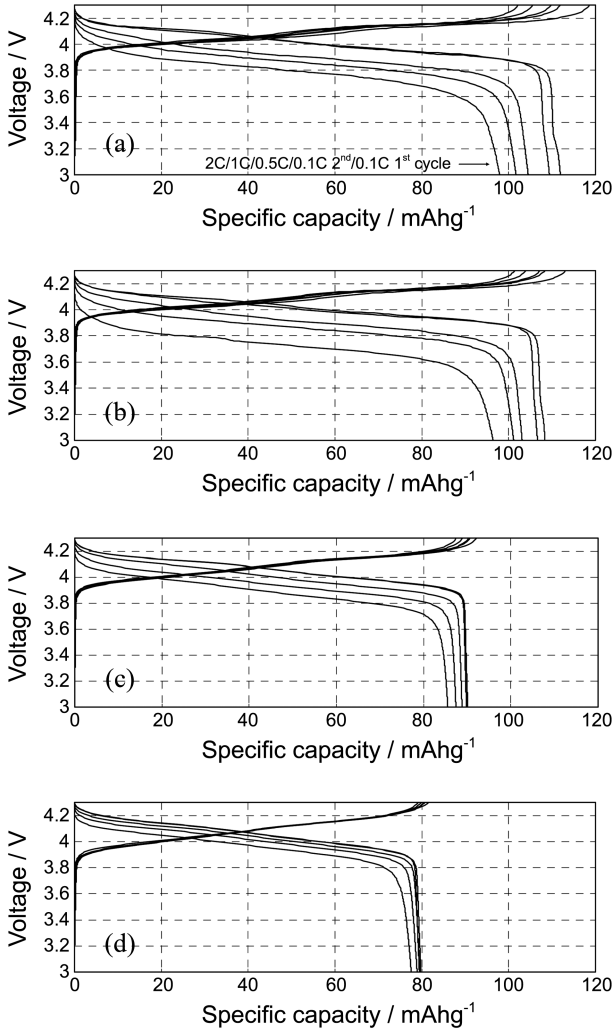

Figure 3. Rate capability of the (a) bare, (b) 1 wt %, (c) 3 wt %, and (d) 5 wt % MnV_2O_6-coated $LiMn_2O_4$ at room temperature.

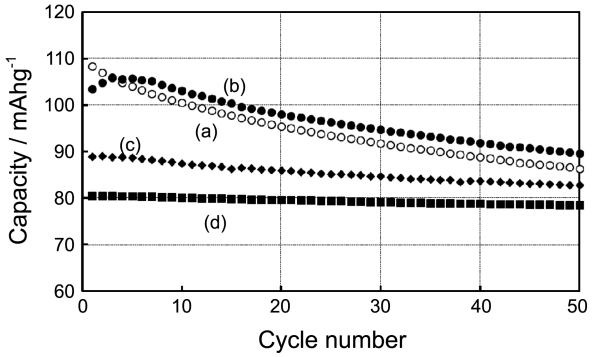

Figure 4. Cycling stability of the (a) bare, (b) 1 wt %, (c) 3 wt %, and (d) 5 wt % MnV_2O_6-coated $LiMn_2O_4$ at 60 °C.

capability of the coated material, a dramatic decrease in discharge capacity would make it impractical to apply the coating more than 3 wt %.

Kim *et al.* investigated the synthesis of MnV_2O_6 and its possible use as an anode material of lithium rechargeable batteries.[19] MnV_2O_6 showed a redox potential at around 1.0 V *vs.* Li^+/Li, which is too low to contribute to the cathode capacity. Although MnV_2O_6 is not an electrochemically inactive material in terms of lithium-ion intercalation, it is expected to behave like an inactive material due to its low redox potential compared to the operating potential of $LiMn_2O_4$ (3.0-4.3 V). In general, the rate capability of $LiMn_2O_4$ can be enhanced by coating with electronic conductive substances or metal doping. Aluminum or magnesium doping has been tried for this purpose.[3,4] Carbon and metals are representative electronic conductive materials that have been applied to improve the rate capability of $LiFePO_4$. However, $LiMn_2O_4$ is prepared in atmospheric condition, which complicates the coating of carbon or metal on $LiMn_2O_4$ due to oxidation of the coating layer. Thus, various conductive metal oxides such as ZnO have been also tried for this purpose.[20]

Two reasons may be postulated to explain the enhanced rate capability in this study. One is the higher electronic conductivity of the coating layer compared to $LiMn_2O_4$. MnV_2O_6 was reported to have an electronic conductivity in the order of 10^{-3} S·cm^{-1}, while that of $LiMn_2O_4$ is around 2 × 10^{-6} S·cm^{-1}.[21,22] The other is the effect of vanadium doping. Doping with a different metal element into the cathode materials is recognized to affect the electronic conductivity.[23,24] Vanadium (V^{5+}) doping changes the proportion of Mn^{3+} to Mn^{4+}, thereby affecting the band gap structure and electronic conductivity of the material. The plateau at 3.2-3.3 V found in the discharge profile of the bare $LiMn_2O_4$ did not appear in that of the coated materials, which indicated that the oxygen deficiency of the $LiMn_2O_4$ was recovered by the coating process at 400 °C. Deng *et al.* have proposed that the non-cubic material formed with the oxygen deficiency deteriorates the rate capability by lowering the electronic conductivity between the spinel microcrystals.[25]

The coating process appears to prevent the formation of the non-cubic impurities by recovering the oxygen deficiency. The rate capability might be improved as the resistance of the electrode is lowered by these reasons.

Figure 4 presents the high temperature (60 °C) cyclability at 0.5C-rate. The bare $LiMn_2O_4$ shows steeper capacity fading than the coated materials. Higher capacity retention was achieved with increasing coating concentration. However, the discharge capacity is far less than that of the bare material when the amount of coating material is more than 3 wt % while the 1 wt % coated material begins to surpass the bare material from the 3rd cycle. The optimum coating amount is not investigated in detail in this study but the coating amount of less than 1 wt % seems to be practical considering that the commercial Li-Mn spinel generally exhibits the discharge capacity of ~105 mAhg^{-1}. Metal oxide coating on $LiMn_2O_4$ has been reported to be helpful in mitigating high temperature capacity fading. Although the mechanism remains controversial, the coating layer appears to contribute to reducing the reactions between the electrolyte and electrode and decreasing the Mn-dissolution. The discharge capacities of the bare, 1, 3 and 5 wt % sample at the 1st cycle are 108.3, 103.5, 88.9 and 80.6 mAhg^{-1}

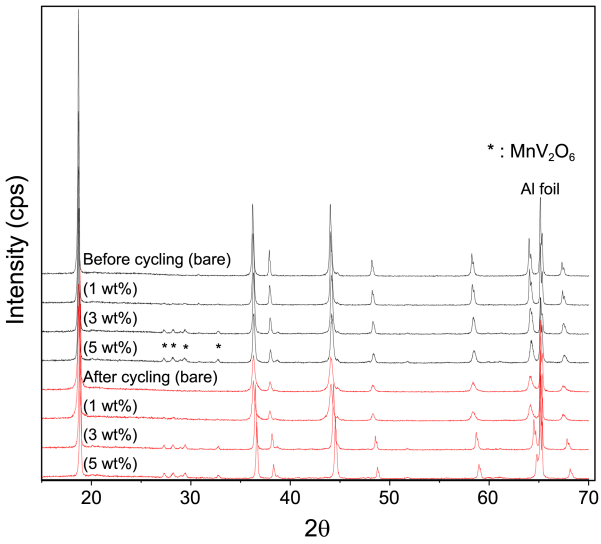

Figure 5. XRD peak patterns of the bare $LiMn_2O_4$ and MnV_2O_6-coated $LiMn_2O_4$ after 50 cycles at 60 °C.

respectively.

The electrodes were analyzed by XRD after 50 cycles to examine the changes in their crystal structure (Fig. 5). The electrodes made of the bare and MnV_2O_6-coated $LiMn_2O_4$ were compared. The peak intensity was lowered for the former but not for the latter, which indicated that the MnV_2O_6 coating layer retained the $LiMn_2O_4$ crystallinity. This lowered intensity seems to be attributed to deformation in the crystal structure arising from the Mn-dissolution. The peaks were shifted apparently to a higher angle after 50 cycles for the electrodes at coating concentrations of 3 and 5 wt %, which represents the contraction of the crystal lattice. The contraction ratio can be calculated as follows.

The contraction ratio was 0.127 and 0.115% for the bare and 1 wt % coated $LiMn_2O_4$, and increased to 0.486 and 1.31% for the 3 and 5 wt % coated samples, respectively when the ratio is calculated according to equation (1). It was somewhat contrary to our expectations that the coating would stabilize the lattice. However, Amatucci *et al.* reported that a small lattice constant of less than 8.21 Å may suppress the disproportionation of Mn^{3+} to Mn^{2+} and Mn^{4+} by increasing the energy required for the disproportionation.[26] We believe that the lattice contraction observed with the MnV_2O_6-coated sample could improve the cyclability by stabilizing the material against the disproportionation.

Conclusion

$LiMn_2O_4$ was coated with MnV_2O_6 *via* a sol-gel coating of V_2O_5. The MnV_2O_6 coating layer was obtained by the heat treatment-induced reaction between V_2O_5 and $LiMn_2O_4$. The presence of the coating layer, confirmed by XRD, SEM, TEM and EDS, contributed to enhancement of the rate capability and high temperature cycle life performance of $LiMn_2O_4$ at the cost of reduced capacity. The improved high temperature cyclability may be attributed to the suppressed Mn-dissolution by blocking the contact between the $LiMn_2O_4$ and the electrolyte. Suppression of the disproportionation of Mn^{3+} to Mn^{2+} and Mn^{4+} in the coated $LiMn_2O_4$ also seems to contribute to improve the cycling stability. The enhanced rate capability resulted from the lowered resistance of the electrode caused by high electric conductivity of the coating layer and the change in the band gap structure by vanadium (V^{5+}) doping into $LiMn_2O_4$.

Acknowledgments. This work was supported by the secondary battery R&D program for leading green industry of MKE/KEIT (No. 10041094, Development of Co-free, high thermal stability and eco-friendly layered cathode material for lithium ion batteries).

References

1. Guyomard, D.; Tarascon, J. M. *J. Power Sources* **1995**, *54*, 92.
2. Xia, Y.; Yoshio, M. *J. Power Sources* **1997**, *66*, 129.
3. Song, D.; Ikuta, H.; Uchida, T.; Wakihira, M. *Solid State Ionics* **1999**, *117*, 151.
4. Gummow, R. J.; Kock, A. de; Thackeray, M. M. *Solid State Ionics* **1994**, *69*, 59.
5. Tu, J.; Zhao, X. B.; Xie, J.; Cao, G. S.; Zhuang, D. G.; Zhu, T. J.; Tu, J. P. *J. Alloys Compd.* **2007**, *432*, 313.
6. Tu, J.; Bao, X. B.; Cao, G. S.; Zhuang, D. G.; Zhu, T. J.; Tu, J. P. *Electrochim. Acta* **2006**, *51*, 6456.
7. Gnanaraj, J. S.; Pol, V. G.; Gedanken, A.; Aurbach, D. *Electrochem. Comm.* **2003**, *5*, 940.
8. Arumugam, D.; Paruthimal, K. G. *J. Electroanal. Chem.* **2008**, *624*, 197.
9. Ha, H.-W.; Yun, N. J.; Kim, K. *Electrochim. Acta*, *Volume* **2007**, *52*, 3236.
10. Tu, J.; Zhao, X. B.; Xie, J.; Cao, G. S.; Zhuang, D. G.; Zhu, T. J.; Tu, J. P. *J. Alloy Compd.*, *Volume* **2007**, *432*, 313.
11. Liu, H.; Cheng, C.; Zongqiuhu, Zhang, K. *Mater. Chem. Phys.* **2007**, *101*, 276.
12. Lim, S.; Cho, J. *Electrochem. Commun.* **2008**, *10*, 1478.
13. Walz, K. A.; Johnson, C. S.; Genthe, J.; Stoiber, L. C.; Zeltner, W. A.; Anderson, M. W.; Thackeray, M. M. *J. Power Sources* **2010**, *195,* 4943.
14. Lee, D. J.; Lee, K. S.; Myung, S. T.; Yashiro, H.; Sun, Y. K. *Journal of Power Sources* **2011**, *196*, 1353.
15. Qing, C.; Bai, Y.; Yang, J.; Zhang, W. *Electrochim. Acta* **2011**, *56*, 6612.
16. Kim, C.-S., *et al. Meeting Abstracts*. No. 3. The Electrochemical Society, 2010.
17. Lee, J.-W.; Park, S.-M.; Kim, H.-J. *J. Power Sources* **2009**, *188*, 583.
18. Dachuan, Y.; Niankan, X.; Jingyu, Z.; Xiulin, Z. *Mater. Res. Bull.* **1996**, *31*, 335.
19. Kim, S.-S.; Ikuta, H.; Wakihara, M. *Solid State Ionics* **2001**, *139*, 57.
20. Liu, H., Cheng, C.; Zhongqiuhu; Zhang, K. *Mater. Chem. Phys.* **2007**, *101*, 276.
21. Gouda, G. M.; Nagendra, C. L. *Sensors Actuators A: Physical* **2009**, *155*, 263.
22. Guan, J.; Liu, M. *Solid State Ionics* **1998**, *110*, 21.
23. Wu, X. M.; He, Z. Q.; Chen, S.; Ma, M. Y.; Xiao, Z. B.; Liu, J. B. *Mater. Lett.* **2006**, *60*, 2497.
24. Son, S. T.; Kim, H. G. *J. Power Sources* **2005**, *147*, 220.
25. Deng, B.; Nakamura, H.; Yoshio, M. *J. Power Sources* **2005**, *141*, 116.
26. Amatucci, G. G.; Pereira, N.; Zheng, T.; Tarascon, J. M. *J. Electrochem. Soc.* **2001**, *148*, A171.